NATIONAL ADVISORY COMMITTEE FOR AERONAUTICS

TECHNICAL NOTE 2423

THEORETICAL AERODYNAMIC CHARACTERISTICS OF BODIES IN A FREE-MOLECULE-FLOW FIELD

By Jackson R. Stalder and Vernon J. Zurick

Ames Aeronautical Laboratory
Moffett Field, Calif.

Washington

July 1951

NATIONAL ADVISORY COMMITTEE FOR AERONAUTICS

TECHNICAL NOTE 2423

THEORETICAL AERODYNAMIC CHARACTERISTICS OF BODIES IN A FREE-MOLECULE-FLOW FIELD

By Jackson R. Stalder and Vernon J. Zurick

SUMMARY

An analytic investigation is made of the aerodynamic coefficients of various bodies located in a free-molecule-flow field. These bodies are the following: flat plate, cylinder, sphere, and cone. Calculations are performed using values of molecular speed ratio (ratio of stream speed to most probable molecular speed) ranging from 0 to 20.

The aerodynamic coefficients of a cone are calculated for angles of attack ranging from 0° to 60°. The semivertex angles of the cones investigated vary from 2.5° to 30°.

The calculations are performed assuming two types of molecular reflection, specular and diffuse; in addition, for the cone, a third type of molecular reflection, wherein impinging molecules are not re-emitted from the body but are swept along its surface, is postulated in order to compare the drag coefficients calculated by free-molecule-flow theory with values obtained from continuum theory.

INTRODUCTION

Consideration of the problem of the flight of high-speed long-range aircraft has indicated that skin temperature and drag forces may be considerably reduced by operation at high altitudes. Consequently, it becomes of interest to determine the aerodynamic forces arising from high-speed flight at high altitudes. Flight at altitudes where the molecular-mean-free path is larger than a characteristic body dimension is in the free-molecule-flow regime. Molecular-mean-free path as a function of altitude is given in reference 1. (At an altitude of 75 miles, the mean-free path is about 1 foot.) Calculations relating skin temperature, altitude, and velocity have previously been completed in reference 1; drag forces, however, were not computed.

Analytic investigations of the drag forces acting on simple body shapes in free-molecule flow have been reported in references 2, 3, and 4, while experimental investigations have been described in references 4 and 5.

In all these analyses, it was assumed that the gas molecules have a Maxwellian distribution of thermal velocity superimposed upon the mass velocity. This assumption is likewise made in the present paper. Heineman (reference 2) and Ashley (reference 3) have calculated the aerodynamic coefficients for various body shapes including the flat plate, sphere, cylinder, and cone. However, the expressions for the drag coefficients of the sphere and cylinder were not integrated by Heineman, while Ashley's solution for the cylinder was not expressed in closed form. Also, in both papers, the drag coefficients for the conical bodies were calculated only for the special case of zero angle of attack. In this paper, the drag coefficients for the sphere and cylinder are expressed in closed form, and the calculations for the drag coefficients for the cones are extended to include angles of attack other than zero. Two types of molecular reflection, diffuse and specular, are investigated. Molecular reflection which occurs in a random direction without relation to the previous velocity direction is termed diffuse reflection. Reflection such that the molecules leave the surface at an angle equal to the angle of incidence is called specular reflection.

As previously stated, free-molecule theory accounts for both the mass motion of the gas and the thermal motion of the molecules. Early investigations of rarefied gas flow were based upon the assumption that the velocity of the molecules was equal to the translatory velocity of the gas, thus neglecting the thermal motion of the molecules. As pointed out by Zahm (reference 6), expressions for the forces acting on various bodies located in a field of such particles were derived by Newton, who assumed that the molecules were either perfectly elastic or perfectly inelastic. A perfectly elastic molecule rebounds after a collision with a surface in such a manner that the n rmal component of velocity is reversed. A perfectly inelastic molecule loses the normal component of velocity upon impact. In both cases, however, the tangential component remains unchanged. In this paper, flow of elastic particles having only a translatory mass motion will be termed "Newtonian flow," and flow of inelastic particles will be termed "inelastic Newtonian flow."

At high flow speeds where molecular thermal velocities become relatively unimportant, the expressions derived from free-molecule-flow theory for the forces on a body for the case of specular reflection reduce to the expressions for a body in a Newtonian flow field.

Inelastic Newtonian flow approximates the condition of continuum hypersonic flow in which the shock wave lies very close to the body. Consequently, impact forces of inelastic Newtonian flow have been applied to an analysis of hypersonic flow (reference 7). In addition to the impact forces of inelastic Newtonian flow, other forces of a centripetal nature exist as a result of flow over curved surfaces. An investigation of the effects of these centripetal forces is also presented in reference 7.

The purpose of this paper is to obtain solutions for the aerodynamic coefficients of various bodies in a free-molecule-flow field and to calculate the lift and drag coefficients for a conical body at an angle of attack, assuming two types of molecular reflection, specular and diffuse. A comparison is then made of the drag coefficient for a cone at zero angle of attack calculated by free-molecule methods, assuming a hypothetical type of molecular reflection similar to that of Newton's inelastic particles, with the drag coefficient tabulated in reference 7 for inelastic Newtonian flow and the drag coefficient calculated in reference 8 for continuum flow.

NOTATION

A surface area, square feet

c_x, c_y, c_z components of total velocity, feet per second

C_i aerodynamic coefficient due to impinging molecules, dimensionless

C_{D_i} drag coefficient due to impinging molecules, dimensionless

C_{L_i} lift coefficient due to impinging molecules, dimensionless

C_r aerodynamic coefficient due to diffuse re-emission of the molecules, dimensionless

C_{D_r} drag coefficient due to diffuse re-emission of the molecules, dimensionless

C_{L_r} lift coefficient due to diffuse re-emission of the molecules, dimensionless

C_D total drag coefficient assuming diffuse re-emission

$(C_{D_i} + C_{D_r})$, dimensionless

C_L total lift coefficient assuming diffuse re-emission

$(C_{L_i} + C_{L_r})$, dimensionless

C_{D_S} total drag coefficient assuming specular reflection of the molecules, dimensionless

C_{L_S} total lift coefficient assuming specular reflection of the molecules, dimensionless

G_i momentum force due to impinging molecules, pounds

G_r normal diffuse re-emission momentum force, pounds

G_S total normal specular momentum force, pounds

I_o modified Bessel function of first kind and zero order

I_1 modified Bessel function of first kind and first order

l_x, l_y, l_z direction cosines in an arbitrary direction, dimensionless (Subscripts l and d refer to lift and drag directions.)

L length, feet

M Mach number, dimensionless

m mass of one molecule, slugs

N number of molecules per unit volume of gas

R radius of body, feet

s molecular speed ratio (ratio of stream mass velocity to most probable molecular speed)

$\left(\frac{U}{V_m} = \sqrt{\frac{\gamma}{2}}\ M\right)$, dimensionless

s_r diffuse re-emission speed ratio

$\left(\frac{U}{V_r}\right)$, dimensionless

U mass velocity, feet per second

U_x, U_y, U_z components of mass velocity, feet per second

V_m most probable molecular speed, feet per second

V_r most probable re-emission speed, feet per second

x, y, z local Cartesian coordinates

α angle of attack of body with respect to free stream

β reciprocal of most probable molecular speed $\left(\frac{1}{V_m}\right)$, seconds per foot

γ ratio of specific heats, dimensionless

δ semivertex angle of cone

θ angle of attack of body element with respect to free stream

ρ density of gas stream, slugs per cubic foot

φ azimuthal angle measured at base of cone

χ dimensionless quantity defined by

$$\chi = \exp\left(-s^2 l_{xd}^2\right) + \sqrt{\pi}\, s\, l_{xd}\left[1 + \operatorname{erf}\left(s\, l_{xd}\right)\right]$$

χ' dimensionless quantity defined by

$$\chi' = \exp\left(-s^2 l_{xd}'^2\right) - \sqrt{\pi}\, s\, l_{xd}'\left[1 - \operatorname{erf}\left(s\, l_{xd}'\right)\right]$$

Ω dimensionless quantity defined by

$$\Omega = \left(l_x \beta U_x + l_y \beta U_y + l_z \beta U_z\right)\left\{\exp\left(-\beta^2 U_x^2\right) + \sqrt{\pi}\,\beta U_x\left[1 + \operatorname{erf}\left(\beta U_x\right)\right]\right\} + \frac{\sqrt{\pi}}{2} l_x\left[1 + \operatorname{erf}\left(\beta U_x\right)\right]$$

Ω' dimensionless quantity defined by

$$\Omega' = \left(l_x' \beta U_x' + l_y' \beta U_y' + l_z' \beta U_z'\right)\left\{\exp\left(-\beta^2 U_x'^2\right) - \sqrt{\pi}\,\beta U_x'\left[1 - \operatorname{erf}\left(B U_x'\right)\right]\right\} - \frac{\sqrt{\pi}}{2} l_x'\left[1 - \operatorname{erf}\left(\beta U_x'\right)\right]$$

erf(a) error function $\frac{2}{\sqrt{\pi}} \int_0^a \exp(-x^2)\, dx$

Superscript

refers to shielded surface only

ANALYSIS

The basic assumptions involved in the formulation of the expressions for the force on a body in a free-molecule-flow field are the following: (1) the gas molecules have a Maxwellian velocity distribution superimposed upon a uniform mass velocity, and (2) collisions between impinging and re-emitted molecules are negligible.

As a result of the second assumption, the total force can be broken down into two components: one arising from the bombardment by impinging molecules and the other arising from the re-emission of the molecules from the surface.

The type of re-emission of the molecules from the body surface can be divided into several categories, the more common of these being diffuse and specular reflection. The phenomenon of molecular reflection is treated in greater detail in references 1 and 9, and only a brief discussion is given here. Diffuse reflection, which is most common physically, occurs in such a manner that all previous directional history is erased, the actual direction of re-emission being controlled by the Knudsen cosine law. The nature of this type of re-emission is such that the molecules, upon leaving the surface, have a Maxwellian distribution of speed which depends upon the temperature of the re-emitted stream. For the case of specular reflection, the molecules leave the surface in a direction determined by the angle of incidence. Thus, the normal component of velocity is reversed, while the tangential component remains unchanged.

The method of calculation of C_i and C_r, the incident and re-emission aerodynamic coefficients, is outlined in reference 4, and is summarized in the following paragraphs.

In the integrals presented below, which are taken from reference 4, the direction cosines between the local coordinate axes of the body surface area and the momentum force are given by l_x, l_y, and l_z. Figure 1 illustrates the coordinate axes for an element of area used in this report. The positive x axis is normal to the element and is directed into the exposed surface. The mass velocity vector makes an angle θ with the positive direction of the y axis. Figures 2 and 3 illustrate

the elements of area chosen for each of the bodies. The components of mass velocity U_x, U_y, and U_z are in the direction of the local axes. The first integral term applies directly to the area exposed to the mass velocity; the second integral term applies to the rear or shielded surface of the body. These areas are taken into account separately because the front of the body acts as a shield preventing collisions of the rear side with all molecules except those having absolute velocity components in the direction of flight with magnitude equal to or greater than the flight speed (reference 1). The shielded area on the surface of a cone is shown in figure 4. Other methods have been devised to account for the shielded area and are presented in references 2 and 3.

Force Due to Impinging Molecules

The component of momentum in a direction defined by l_x, l_y, and l_z imparted to a differential plane area in a free-molecule-flow field by the impact of impinging molecules is

$$dG_i = \frac{\beta^3 mN}{\pi^{3/2}} \left[\int_{-\infty}^{\infty}\int_{-\infty}^{\infty}\int_{0}^{\infty} c_x(l_x c_x + l_y c_y + l_z c_z) \exp\left\{-\beta^2\left[(c_x - U_x)^2 + (c_y - U_y)^2 + (c_z - U_z)^2\right]\right\} dc_x\, dc_y\, dc_z - \int_{-\infty}^{\infty}\int_{-\infty}^{\infty}\int_{-\infty}^{0} c_x(l_x c_x + l_y c_y + l_z c_z) \exp\left\{-\beta^2\left[(c_x - U_x)^2 + (c_y - U_y)^2 + (c_z - U_z)^2\right]\right\} dc_x\, dc_y\, dc_z \right] dA \qquad (1)$$

or

$$dG_i = \frac{\rho U^2}{2} \frac{1}{\sqrt{\pi}\, s^2} \left\{ \left[(l_x \beta U_x + l_y \beta U_y + l_z \beta U_z) \left\{ \sqrt{\pi}\, \beta U_x \left[1 + \operatorname{erf} (\beta U_x) \right] + \exp (-\beta^2 U_x^2) \right\} + \frac{\sqrt{\pi}}{2} l_x \left[1 + \operatorname{erf} (\beta U_x) \right] \right] - \left[(l_x \beta U_x + l_y \beta U_y + l_z \beta U_z) \left\{ \sqrt{\pi}\, \beta U_x \left[1 - \operatorname{erf} (\beta U_x) \right] - \exp (-\beta^2 U_x^2) \right\} + \frac{\sqrt{\pi}}{2} l_x \left[1 - \operatorname{erf} (\beta U_x) \right] \right] \right\} dA \qquad (2)$$

where $\rho = mN$ and $\beta = 1/V_m = s/U$.

The choice of the direction cosines is related to the component of force being computed. If the drag is being calculated, it is necessary to find the direction angles between each of the local axes and the direction of drag. Likewise, direction angles are found for any other force component being investigated.

In applying equation (2) to arbitrary bodies, the momentum force in a desired direction due to the impinging molecules is first found for an element of area of the body under investigation. When this relationship is used, an integration over the surface area of the body gives the desired momentum force on the entire body due to impinging molecules. The incident aerodynamic coefficient referred to a characteristic body area is then found.

Force Due to Diffuse Molecular Reflection

For the case of diffuse molecular reflection, the normal re-emission force on the front side of a differential area inclined to the direction of flow is given by

$$dG_r = \frac{\rho U^2}{2} \frac{\chi}{2 s s_r} dA \qquad (3)$$

and the normal re-emission force on the rear side is given by

$$dG_r' = \frac{\rho U^2}{2} \frac{\chi'}{2 s s_r} dA \qquad (4)$$

The difference obtained by subtraction of equation (4) from equation (3) is the total re-emission force. (See appendix A, reference 4.)

The value of s_r is a complicated function of the surface condition of the body; however, in this paper, s_r is assumed equal to s for all calculations. At low flow speeds, this assumption is very nearly correct. At high flow speeds, however, the value of s_r is less than that of s.

The resolution of the normal force of equations (3) and (4) into the lift and drag components followed by integration over the body surface gives the re-emission lift and drag acting on the body. After calculation of the lift and drag, the aerodynamic coefficients for diffuse molecular reflection can be found.

Force Due to Specular Molecular Reflection

For the case of specular reflection, the molecules leave the surface in a direction determined by the angle of incidence. Since the reflection angle is equal to the angle of incidence, the normal component of velocity is reversed, while the tangential component remains unchanged. Therefore, the momentum change is in a direction normal to the bombarded surface, and the total momentum force consists of two equal components: one due to impingement of the molecules, the other due to the reflection of the molecules from the surface.

The incident momentum force on a differential area in a direction normal to the surface is found from equation (2) by the substitution of the following direction cosines:

$$\begin{aligned} l_x &= \cos 0 = 1 \\ l_y &= \cos \frac{\pi}{2} = 0 \\ l_z &= \cos \frac{\pi}{2} = 0 \end{aligned} \tag{5}$$

The total normal momentum force for the case of specular reflection is twice as great as the incident normal force, and it is given by

$$dG_S = \frac{\rho U^2}{2} \frac{2}{\sqrt{\pi}\, s} \left[\left\{ \sqrt{\pi} \left[1 + \operatorname{erf}(\beta U_x) \right] \left(\beta^2 U_x^2 + \frac{1}{2} \right) + \beta U_x \exp(-\beta^2 U_x^2) \right\} - \left\{ \sqrt{\pi} \left[1 - \operatorname{erf}(\beta U_x) \right] \left(\beta^2 U_x^2 + \frac{1}{2} \right) - \beta U_x \exp(-\beta^2 U_x^2) \right\} \right] dA \tag{6}$$

Integration of equation (6) over the surface of the body after the normal force has been resolved into the lift and drag components yields the total lift and drag on the body due to specular reflection.

Force Due to Molecular Reflection Analogous to Hypersonic Flow

A third type of molecular reflection is postulated here in order to approximate the characteristics of hypersonic flow over a body. This type of reflection is much like that of Newton's inelastic particles, the only difference being that thermal velocities are considered. It is assumed that the molecules flow along the body after collision with the surface; thus, the normal component of velocity is destroyed while the tangential component remains unchanged. The values of the aerodynamic coefficients thus obtained are one-half the values calculated for specular reflection. This type of molecular reflection is extremely unlikely and probably physically impossible; however, the justification for this assumption lies in the fact that the conditions of hypersonic continuum flow over a body are approximated. In continuum flow, the stream follows the surface of the body. As the flow speed increases, the zone of influence of the body on the gas stream approaches the surface of the body until the shock wave lies nearly on the body surface. On the basis of the above assumption, free-molecule theory is compared with continuum theory.

The expressions for the aerodynamic coefficients of a flat plate, cylinder, sphere, and cone together with the details of the development are presented in the appendix.

DISCUSSION AND RESULTS

Flat Plate

The aerodynamic coefficients for a flat plate inclined at various angles of attack to the direction of mass flow were calculated for values of molecular speed ratio varying from 0 to 20 and are presented in figures 5, 6, and 7.

The limiting values, as the molecular speed ratio approaches infinity, of the aerodynamic coefficients for a flat plate for the case of specular reflection reduce to the classical expressions for Newtonian flow, mentioned by Zahm (reference 6)

$$C_{D_S} = 4 \sin^3 \alpha$$

$$C_{L_S} = 4 \sin^2 \alpha \cos \alpha$$

A comparison of the drag coefficients for diffuse and specular reflection indicates that the value for diffuse reflection has a larger value at low angles of attack; at the high angles of attack, the specular drag coefficient is greater. This is explained by the fact that, at small angles of attack, the drag for the case of specular reflection is due to the small normal component of velocity; whereas the drag for the case of diffuse reflection has a value which results from the loss of both a small normal velocity component and a large tangential velocity. At large angles of attack, the re-emission velocity arising from diffuse reflection is less than the re-emission velocity due to specular reflection, while the momentum effects of the incident molecules are nearly the same for both cases. Thus, the total drag coefficient due to specular reflection is greater. This last point is made clear by considering a flat plate at a 90° angle of attack.

The lift-drag ratios for the plate are shown in figure 6. The expression for the lift-drag ratio for specular reflection is $\cot \alpha$. Obviously, these values have a great range. The aerodynamic coefficients for double-wedge wings can easily be found by modifying the coefficients for the flat plate. The low values for diffuse reflection are notable.

Cylinder

Values of the total drag coefficient for the case of diffuse reflection were obtained from reference 4 and are presented in figure 8. An analytical expression for s_r employed in the calculations of reference 4 was found by means of an energy and mass balance over the surface of the cylinder taking into account conditions which exist at the surface of the cylinder. Details of the calculations can be found in appendix A, reference 4.

A recent experimental investigation of drag (reference 4) has supplied the drag-coefficient data plotted in figure 8. Theoretical curves of the drag coefficient for both diffuse and specular reflection are plotted for comparison with the experimental data. A complete discussion of the comparison of the experimental data and the curve representing diffuse reflection can be found in reference 4. In addition, a curve of the drag coefficient for the case of diffuse reflection, which includes the assumption that the molecular speed after impact is the same as that before impact, is shown for comparison with the drag coefficient obtained from reference 4. The curves agree well at the low speeds, but diverge as the molecular speed ratio increases.

Sphere

The results of the calculations for the drag coefficient for a sphere are presented in figure 9. The drag coefficient for the case of diffuse reflection is compared with the drag coefficient for the case of specular reflection. The value of the drag coefficient for diffuse reflection lies above the value for specular reflection but both curves asymptotically approach the limiting value of 2 at large values of s.

The investigation into the case of specular reflection for a sphere yields an interesting result. Equations (A15) and (A19) indicate that the total drag due to the specular type of reflection has the same value as the drag caused by molecules striking the surface and coming to rest; that is, the integrated effect of the re-emission drag arising from specular reflection of the molecules from the surface is zero. It should be noted that the sphere is unique in that the re-emission momentum force of the molecules reflected in a forward direction is equal and opposite to the momentum force of the molecules reflected in the direction of the mass flow.

Cones

Calculations for the drag and lift coefficients of the various cones, assuming three types of molecular reflection, are shown in figures 10, 11, 12, 13, and 14.

Results considering diffuse reflection.- Figure 10 gives the drag coefficient, $C_D = C_{D_i} + C_{D_r}$, for the case of diffuse molecular reflection. It is interesting to note that the drag coefficients for the sharp cones are higher than those for the blunt cones. The impinging molecules lose both the tangential and normal components of velocity. The tangential or friction force on the greater exposed surface area of the sharp cones is greater than the tangential force on the blunt cones. Hence, the drag coefficients are large for the sharp cones since the reference area is the same base area for all cones.

The lift coefficient, $C_L = C_{L_i} + C_{L_r}$, is plotted in figure 11. The lift coefficient for blunt cones at large angles of attack decreases as molecular speed ratio becomes small. This is due to the collision of the top or shielded surface of the cone with molecules possessing an absolute velocity in the direction of flight with magnitude equal to or greater than the flight speed. The momentum force due to these molecules is then in a direction opposite to the direction of lift.

At low values of molecular speed ratio, in the range where the thermal velocity is equal to or greater than the mass velocity, the contribution of the thermal velocity to the absolute velocity becomes a determining factor in the calculation of the aerodynamic coefficients; whereas, at high values of molecular speed ratio, the contribution of the thermal velocity is negligible.

Results considering specular reflection.- Figures 12 and 13 give the drag and lift coefficients for cones for the case of specular reflection. At small angles of attack, the drag coefficients of the blunt cones have higher values than those of the sharp cones. The reverse is true at large angles of attack. A very sharp cone at zero angle of attack has very little drag because the change in momentum of the molecules has only a very small component in the direction of drag. This component, acting on a blunt cone, is much greater. At a high angle of attack, the surface area exposed to the flow by the sharp cones exceeds the exposed surface area of the blunt cones, for equal base areas, and hence the drag force is greater for the sharp cones. Since the drag coefficients are referred to the same base area rather than a projection of the exposed area, they must vary in direct proportion to the drag force.

Results considering an approximation of continuum theory.- The values of the lift and drag coefficients obtained by means of the hypothetical type of re-emission postulated in the analysis are half the values obtained for the case of purely specular reflection in which the normal component of velocity is reversed as a molecule leaves the surface.

Values of drag coefficients for cones in continuum flow have been calculated by Kopal (reference 8). Likewise, reference 7 describes an investigation of continuum flow at hypersonic speed. In figure 14, the drag coefficient of a 30° semivertex angle cone, at zero angle of attack, calculated for the above hypothetical case of molecular reflection, is compared with the drag coefficient calculated in references 7 and 8.

Experimental values for the drag coefficient of a 30° semivertex cone-cylinder fired in the Ames supersonic free-flight tunnel (reference 10) are also shown in figure 14 for comparison with the analytic values. The experimental values include head drag on the cone, friction drag on the cylindrical afterbody, and base drag. The free-molecule values take into account head drag on a 30° semivertex angle cone only. At high values of flow speed, the drag coefficient values obtained from free-molecule theory approach the values for inelastic Newtonian flow. Although the analysis of reference 7 for flow past a cone takes into account centrifugal forces arising from flow over curved surfaces, the expression for the drag coefficient reduces to that for inelastic Newtonian flow at zero angle of attack where the centrifugal forces are

zero. The drag coefficient due to inelastic Newtonian flow is represented in figure 14 by a straight line, since it is independent of flow speed.

In figure 14, the agreement between free-molecule-flow theory and the experimental data for a continuum flow at low values of molecular speed ratio is entirely fortuitous. The increase in the value of the drag coefficient calculated from free-molecule-flow theory is due to the fact that the drag force is proportional to the first power of the velocity at low speeds; whereas the increase in the value of the experimental drag coefficient is the characteristic rise which occurs in the transonic range of stream speeds in continuum flow.

CONCLUDING REMARKS

The lift-drag ratios of a flat plate in free-molecule flow are very small for the case of diffuse molecular reflection. The lift-drag ratios decrease as the molecular speed ratio is increased. At high speeds, the lift-drag ratios for the flat plate are more favorable at small angles of attack than at large angles of attack.

For the case of diffuse molecular reflection, the lift and drag coefficients of all the bodies investigated approach constant limiting values at high speeds. These limiting values depend upon the body geometry and the angle of attack. At low speeds, the drag coefficients for all the bodies approach an infinite value; this is due to the fact that the drag force is proportional to the first power of the velocity at low speeds.

For the case of specular reflection, the aerodynamic coefficients of all the bodies investigated likewise approach constant limiting values at high speeds. These limiting values correspond to those calculated by means of inelastic Newtonian flow theory.

Ames Aeronautical Laboratory
National Advisory Committee for Aeronautics
Moffett Field, Calif., May 9, 1951.

APPENDIX

DERIVATION OF THE AERODYNAMIC COEFFICIENTS FOR BODIES IN A FREE-MOLECULE-FLOW FIELD

The details of the development for the lift and drag coefficients for the various bodies are given below:

Flat Plate

The combined form of equation (2) is.

$$dG_i = \frac{\rho U^2}{2} \frac{1}{\sqrt{\pi}\, s^2} \left\{ 2 \left(l_x \beta U_x + l_y \beta U_y + l_z \beta U_z \right) \left[\sqrt{\pi}\, \beta U_x \operatorname{erf}(\beta U_x) + \exp(-\beta^2 U_x^2) \right] + \sqrt{\pi}\, l_x \operatorname{erf}(\beta U_x) \right\} dA \qquad (A1)$$

Since the faces of a flat plate are parallel, the same direction cosines apply to both the front and rear surfaces and the momentum of the molecules striking both faces can be collectively taken into account, and equation 2 written in the combined form is applicable. This is not true for an element of area chosen for the cone, however, and the combined form of equation (2) cannot be used for that case. For the case of the flat plate, equation (A1) gives the incident momentum force on both sides of the plate, and the aerodynamic coefficients can be found without further integration.

The direction cosines and velocity components are the following:

$$\left.\begin{array}{lll} l_{xd} = \sin\alpha & l_{xl} = \cos\alpha & U_x = U \sin\alpha \\ l_{yd} = -\cos\alpha & l_{yl} = \sin\alpha & U_y = -U \cos\alpha \\ l_{zd} = 0 & l_{zl} = 0 & U_z = 0 \\ & \beta U = s & \end{array}\right\} \qquad (A2)$$

Substitution of the relations of equation (A2) into equation (A1) gives the following coefficients, referred to the area of one side of the plate.

$$C_{D_i} = \frac{2}{\sqrt{\pi}\, s} \exp\left(-s^2 \sin^2\alpha\right) + 2 \sin\alpha \left(1 + \frac{1}{2s^2}\right) \operatorname{erf}(s \sin\alpha) \quad \text{(A3)}$$

$$C_{l_i} = \frac{\cos\alpha}{s^2} \operatorname{erf}(s \sin\alpha) \quad \text{(A4)}$$

The normal force due to diffuse molecular re-emission from both front and rear surfaces is given by the difference between equations (3) and (4).

$$dG_r - dG_r' = \frac{\rho U^2}{2} \frac{1}{2 s s_r} (X - X') \, dA \quad \text{(A5)}$$

Substitution of $U \sin\alpha$ for U_x and s for βU in X and X' reduces equation (A5) to

$$dG_r - dG_r' = \frac{\rho U^2}{2} \frac{\sqrt{\pi} \sin\alpha}{s_r} \, dA \quad \text{(A6)}$$

The re-emission drag force on an element of area is

$$\frac{\rho U^2}{2} \frac{\sqrt{\pi} \sin^2\alpha}{s_r} \, dA$$

and

$$C_{D_r} = \frac{\sqrt{\pi} \sin^2\alpha}{s_r} \quad \text{(A7)}$$

The total drag coefficient is then

$$C_D = \frac{2}{\sqrt{\pi}\, s} \exp\left(-s^2 \sin^2\alpha\right) + 2 \sin\alpha \left(1 + \frac{1}{2s^2}\right) \operatorname{erf}(s \sin\alpha) + \frac{\sqrt{\pi} \sin^2\alpha}{s_r}$$

The lift due to molecular re-emission on an element of area is

$$\frac{\rho U^2}{2} \frac{\sqrt{\pi} \sin\alpha \cos\alpha}{s_r} \, dA$$

and

$$C_{L_r} = \frac{\sqrt{\pi} \sin\alpha \cos\alpha}{s_r} \quad \text{(A8)}$$

The total lift coefficient is then

$$C_L = \frac{\cos\alpha}{s^2} \operatorname{erf}(s \sin\alpha) + \frac{\sqrt{\pi} \sin\alpha \cos\alpha}{s_r}$$

For the case of specular reflection, the total momentum force in a direction normal to the surface resulting from incident and reflected molecules on both sides of a flat plate is

$$dG_S = \frac{\rho U^2}{2} \frac{2}{\sqrt{\pi}\, s} \left[2\beta U_x \exp(-\beta^2 U_x^2) + 2\sqrt{\pi} \left(\beta^2 U_x^2 + \frac{1}{2} \right) \operatorname{erf}(\beta U_x) \right] dA \tag{A9}$$

from equation (6).

The drag and lift coefficients are then found after resolving the normal force as given in equation (A9) intc drag and lift components.

$$C_{D_S} = \sin\alpha \left[\frac{4}{\sqrt{\pi}\, s} \sin\alpha \exp(-s^2 \sin^2\alpha) + 4 \left(\sin^2\alpha + \frac{1}{2s^2} \right) \operatorname{erf}(s \sin\alpha) \right] \tag{A10}$$

$$C_{L_S} = \cos\alpha \left[\frac{4}{\sqrt{\pi}\, s} \sin\alpha \exp(-s^2 \sin^2\alpha) + 4 \left(\sin^2\alpha + \frac{1}{2s^2} \right) \operatorname{erf}(s \sin\alpha) \right] \tag{A11}$$

Cylinder

The case of diffuse molecular reflection on a transverse cylinder has been investigated in reference 4, and the total drag coefficient based on the projected area of the cylinder is

$$C_D = \frac{\sqrt{\pi}}{s} \exp\left(-\frac{s^2}{2}\right) \left\{ I_o\left(\frac{s^2}{2}\right) + \frac{(1+2s^2)}{2} \left[I_o\left(\frac{s^2}{2}\right) + I_1\left(\frac{s^2}{2}\right) \right] \right\} + \frac{\pi^{3/2}}{4 s_r}$$

The specular case only remains to be considered here. The element of area is chosen as shown in figure 2, thus

$$dA = L\, R\, d\,\theta$$

$$l_{xd} = \sin\theta \qquad U_x = U \sin\theta$$

$$l_{yd} = -\cos\theta \qquad U_y = -U \cos\theta$$

$$l_{zd} = 0 \qquad U_z = 0$$

Each element of area is considered to have a rear or shielded area and the normal force on the cylinder is found from equation (A9).

$$dG_S = \frac{\rho U^2}{2} \frac{4LR}{\sqrt{\pi}\, s^2} \left[2s \sin\theta \exp(-s^2\sin^2\theta) + 2\sqrt{\pi} \left(s^2\sin^2\theta + \frac{1}{2} \right) \operatorname{erf}(s \sin\theta) \right] d\theta$$

The drag force is

$$\frac{\rho U^2}{2} \frac{4LR}{\sqrt{\pi}\, s^2} \int_0^{\pi/2} \sin\theta \left[2s \sin\theta \exp(-s^2\sin^2\theta) + 2\sqrt{\pi} \left(s^2\sin^2\theta + \frac{1}{2} \right) \operatorname{erf}(s \sin\theta) \right] d\theta \qquad \text{(A12)}$$

The integrals are

$$\int_0^{\pi/2} \sin^2\theta \exp(-s^2\sin^2\theta)\, d\theta = \frac{\pi}{4} \exp\left(-\frac{s^2}{2}\right) \left[I_0\left(\frac{s^2}{2}\right) - I_1\left(\frac{s^2}{2}\right) \right]$$

$$\int_0^{\pi/2} \sin\theta \operatorname{erf}(s \sin\theta)\, d\theta = \frac{\sqrt{\pi}\, s}{2} \exp\left(-\frac{s^2}{2}\right) \left[I_0\left(\frac{s^2}{2}\right) + I_1\left(\frac{s^2}{2}\right) \right]$$

$$\int_0^{\pi/2} \sin^3\theta \operatorname{erf}(s \sin\theta)\, d\theta = \frac{\sqrt{\pi}\, s}{6} \exp\left(-\frac{s^2}{2}\right) \left[2I_0\left(\frac{s^2}{2}\right) + \left(2 + \frac{1}{s^2}\right) I_1\left(\frac{s^2}{2}\right) \right]$$

and the drag coefficient due to specular reflection, referred to the frontal projected area, is

$$C_{D_S} = \frac{2\sqrt{\pi}}{3s} \exp\left(-\frac{s^2}{2}\right) \left[(3+2s^2)\, I_0\left(\frac{s^2}{2}\right) + (1+2s^2)\, I_1\left(\frac{s^2}{2}\right) \right] \qquad \text{(A13)}$$

Sphere

As shown in figure 2, the element of area for the sphere is given by

$$dA = 2\pi R^2 \cos\theta\, d\theta$$

Equation (A1) for the incident momentum drag force is

$$dG_i = \frac{\rho U^2}{2} (\pi R^2) \frac{2 \cos\theta}{\sqrt{\pi}\, s^2} \left[2s \exp(-s^2 \sin^2\theta) + \sqrt{\pi} \sin\theta \,(2s^2 + 1) \operatorname{erf}(s \sin\theta) \right] d\theta \qquad (A14)$$

The integrals are

$$\int_0^{\pi/2} s \cos\theta \exp(-s^2\sin^2\theta)\, d\theta = \frac{\sqrt{\pi}}{2} \operatorname{erf}(s)$$

$$\int_0^{\pi/2} \cos\theta \sin\theta \operatorname{erf}(s \sin\theta)\, d\theta = \frac{\exp(-s^2)}{2\sqrt{\pi}\, s} + \frac{\left(1 - \frac{1}{2s^2}\right)}{2} \operatorname{erf}(s)$$

and the incident drag coefficient, referred to the frontal projected area, is

$$C_{D_S} = \frac{2s^2+1}{\sqrt{\pi}\, s^3} \exp(-s^2) + \frac{(4s^4 + 4s^2 - 1)}{2s^4} \operatorname{erf}(s) \qquad (A15)$$

The drag force due to molecular re-emission, from equation (A6), is

$$\frac{\rho U^2}{2} \pi R^2 \int_0^{\pi/2} \frac{2\sqrt{\pi}}{s_r} \sin^2\theta \cos\theta \, d\theta \qquad (A16)$$

Integration of equation (A16) yields the re-emission drag coefficient

$$C_{D_r} = \frac{2\sqrt{\pi}}{3 s_r} \qquad (A17)$$

The total drag is given, for diffuse reflection, by

$$C_D = \frac{2 \exp(-s^2)}{\sqrt{\pi}\, s} \left(1 + \frac{1}{2s^2}\right) + 2\left(1 + \frac{1}{s^2} - \frac{1}{4s^4}\right) \operatorname{erf}(s) + \frac{2\sqrt{\pi}}{3 s_r}$$

The drag force due to specular reflection on the sphere is given by

$$\frac{\rho U^2}{2} \pi R^2 \int_0^{\pi/2} \frac{4 \cos\theta \sin\theta}{\sqrt{\pi}\, s^2} \left[2s \sin\theta \exp(-s^2\sin^2\theta) + 2\sqrt{\pi} \left(s^2 \sin^2\theta + \frac{1}{2} \right) \operatorname{erf}(s \sin\theta) \right] d\theta \qquad (A18)$$

The integrals are

$$\int_0^{\pi/2} \cos\theta \sin^2\theta \exp(-s^2\sin^2\theta)\, d\theta = \frac{\sqrt{\pi}}{4s^3}\operatorname{erf}(s) - \frac{\exp(-s^2)}{2s^2}$$

$$\int_0^{\pi/2} \cos\theta \sin\theta \operatorname{erf}(s\sin\theta)\, d\theta = \frac{\exp(-s^2)}{2\sqrt{\pi}\, s} + \left(\frac{2s^2-1}{4s^2}\right)\operatorname{erf}(s)$$

$$\int_0^{\pi/2} \cos\theta \sin^3\theta \operatorname{erf}(s\sin\theta)\, d\theta = \frac{2s^2+3}{8\sqrt{\pi}s^3}\exp(-s^2) + \frac{4s^4-3}{16s^4}\operatorname{erf}(s)$$

and the drag coefficient due to specular reflection, referred to the frontal projected area, is

$$C_{D_S} = \frac{2s^2+1}{\sqrt{\pi}\, s^3}\exp(-s^2) + \left(\frac{4s^4+4s^2-1}{2s^4}\right)\operatorname{erf}(s) \qquad (A19)$$

Cone

Special attention must be given to the conical body. Two separate cases must be investigated, depending on the relationship of the angle of attack of the cone and the semivertex angle of the cone. At an angle of attack less than or equal to the semivertex angle, the entire surface area is exposed to the mass velocity, and the total momentum force is evaluated by a single integration. For those instances where the angle of attack exceeds the semivertex angle, a portion of the surface area is shielded from the mass velocity, and two separate integrations, one for the frontal exposed area and one for the shielded area, are necessary to compute the momentum force. Aerodynamic coefficients are then found referred to the base area of the cone. The element of area chosen for constant angle of attack as shown in figure 3 is given by

$$dA = \frac{\tan\delta}{\cos\delta}\frac{L^2}{2}\, d\varphi$$

Case I – Angle of attack less than or equal to the semivertex angle.– The aerodynamic coefficient due to impinging molecules referred to the base area of the cone is given by (from the first term of equation (2))

$$C_l = \frac{1}{\pi^{3/2} s^2 \sin \delta} \int_0^{\pi} \Omega d\varphi \tag{A20}$$

where

$$\Omega = \left(l_x \beta U_x + l_y \beta U_y + l_z \beta U_z\right) \left\{ \exp(-\beta^2 U_x^2) + \sqrt{\pi}\, \beta U_x \left[1 + \operatorname{erf}(\beta U_x)\right] \right\} + \frac{\sqrt{\pi}\, l_x}{2} \left[1 + \operatorname{erf}(\beta U_x)\right] \tag{A21}$$

Substitution of the appropriate direction cosines into equation (A20) yields the corresponding lift or drag coefficient.

For drag the direction cosines are

$$\left.\begin{aligned} l_{xd} &= \cos \alpha \sin \delta - \sin \alpha \cos \delta \cos \varphi \\ l_{yd} &= -\cos \alpha \sin \delta - \sin \alpha \sin \delta \cos \varphi \\ l_{zd} &= \sin \alpha \sin \varphi \end{aligned}\right\} \tag{A22}$$

and for lift the direction cosines are

$$\left.\begin{aligned} l_{xl} &= -\sin \alpha \sin \delta - \cos \alpha \cos \delta \cos \varphi \\ l_{yl} &= \sin \alpha \cos \delta - \cos \alpha \sin \delta \cos \varphi \\ l_{zl} &= \cos \alpha \sin \varphi \end{aligned}\right\} \tag{A23}$$

The expressions for the several velocity components are the following:

$$\left.\begin{aligned} U_x &= U(\cos \alpha \sin \delta - \sin \alpha \cos \delta \cos \varphi) \\ U_y &= -U(\cos \alpha \cos \delta + \sin \alpha \sin \delta \cos \varphi) \\ U_z &= U \sin \alpha \sin \varphi \end{aligned}\right\} \tag{A24}$$

At zero angle of attack, equation (A20) reduces to a readily integrable expression and the aerodynamic coefficients for this case are

$$C_{D_i} = \frac{s \exp(-s^2\sin^2\delta) + \sqrt{\pi} \sin \delta \left(s^2 + \frac{1}{2}\right) \left[1 + \operatorname{erf}(s \sin \delta)\right]}{\sqrt{\pi}\, s^2 \sin \delta} \tag{A25}$$

and

$$C_{L_i} = 0$$

The lift and drag coefficients due to diffuse molecular reflection are found, from equation (3), to be

$$C_{D_r} = \frac{1}{2\pi s s_r \sin \delta} \int_0^{\pi} l_{xd}\, \chi d\varphi \tag{A26}$$

and

$$C_{L_r} = \frac{1}{2\pi s s_r \sin \delta} \int_0^{\pi} l_{x l}\, \chi d\varphi \tag{A27}$$

At zero angle of attack,

$$C_{D_r} = \frac{\chi}{2 s s_r} \tag{A28}$$

and

$$C_{L_r} = 0$$

The following relations hold for the total lift and drag coefficients for the case of specular reflection:

$$C_{D_S} = \frac{2}{\pi^{3/2} s^2 \sin \delta} \int_0^{\pi} l_{xd} \left\{ \beta U \exp(-\beta^2 U_x^2) + \sqrt{\pi} \left[1 + \operatorname{erf}(\beta U_x)\right] \left(\beta^2 U_x^2 + \frac{1}{2}\right) \right] d\varphi \tag{A29}$$

and

$$C_{L_S} = \frac{2}{\pi^{3/2} s^2 \sin \delta} \int_0^{\pi} l_{xl} \left\{ \beta U_x \exp(-\beta^2 U_x^2) + \sqrt{\pi} \left[1 + \operatorname{erf}(\beta U_x) \right] \left(\beta^2 U_x^2 + \frac{1}{2} \right) \right\} d\varphi \tag{A30}$$

For zero angle of attack

$$C_{D_S} = \frac{2 \sin \delta}{\sqrt{\pi}\, s} \exp(-s^2 \sin^2 \delta) + 2 \left(\sin^2 \delta + \frac{1}{2s^2} \right) \left[1 + \operatorname{erf}(s \sin \delta) \right] \tag{A31}$$

and

$$C_{L_S} = 0$$

Case II — Angle of attack greater than the semivertex angle.— In this case, part of the surface area is shielded from the main flow. This shielded area is bounded by straight-line elements of the cone and, at these boundaries, the flow is tangent to the surface of the cone; that is, the component of velocity in a direction normal to the surface is zero.

From equation (A24)

$$U_x = U(\cos \alpha \sin \delta - \sin \alpha \cos \delta \cos \varphi_1) = 0$$

$$\text{at } \varphi = \varphi_1 \tag{A32}$$

and

$$\varphi_1 = \cos^{-1} \frac{\tan \delta}{\tan \alpha}$$

where φ_1 denotes the boundary line between the exposed and shielded surface areas and is measured around the cone from the vertical as shown in figure 4.

The total incident momentum for the entire surface area is

$$C_{i} = \frac{\rho U^2}{2} \frac{L^2 \tan \delta}{\sqrt{\pi}\, s^2 \cos \delta} \left\{ \int_0^{\varphi_1} \left[(l_x' \beta U_x' + l_y' \beta U_y' + l_z' \beta U_z') \left\{ \exp(-\beta^2 U_x'^2) - \sqrt{\pi}\, \beta U_x' \left[1 - \operatorname{erf}(\beta U_x')\right] \right\} - \frac{\sqrt{\pi}}{2} l_x' \left[1 - \operatorname{erf}(\beta U_x')\right] \right] d\varphi + \int_{\varphi_1}^{\pi} \left\{ (l_x \beta U_x + l_y \beta U_y + l_z \beta U_z) \left\{ \exp(-\beta^2 U_x^2) + \sqrt{\pi}\, \beta U_x \left[1 + \operatorname{erf}(\beta U_x)\right] \right\} + \frac{\sqrt{\pi}}{2} l_x \left[1 + \operatorname{erf}(\beta U_x)\right] \right\} d\varphi \right\} \tag{A33}$$

where

$$\left.\begin{aligned} l_x' &= -l_x & U_x' &= -U_x \\ l_y' &= l_y & U_y' &= U_y \\ l_z' &= -l_z & U_z' &= -U_z \end{aligned}\right\} \tag{A34}$$

A change in the coordinate axis of the element of area on the shielded surface of the cone is the reason for the use of the primed quantities. The positive direction of the x axis for the exposed area is into the surface; whereas the positive direction of the x axis for the shielded area is out of the surface. Since the direction cosines have been derived for the exposed area, reversal of the x axis over the shielded area results in the negative quantities. For the previous bodies considered, this procedure was unnecessary since both front and rear areas were jointly taken into account.

The solution of equation (A33), for the incident aerodynamic coefficient referred to the base area, yields

$$C_i = \frac{1}{\pi^{3/2} s^2 \sin \delta} \left(\int_0^{\varphi_1} \Omega' d\varphi + \int_{\varphi_1}^{\pi} \Omega d\varphi \right) \tag{A35}$$

where Ω and Ω' are the integrands of equation (A33). Either the lift or drag coefficients can be calculated by substituting the appropriate direction cosines.

The re-emission drag and lift coefficients for diffuse reflection are

$$C_{D_r} = \frac{1}{2\pi s s_r \sin \delta} \left(- \int_0^{\varphi_1} l_{xd}' X' d\varphi + \int_{\varphi_1}^{\pi} l_{xd} X d\varphi \right) \tag{A36}$$

and

$$C_{L_r} = \frac{1}{2\pi s s_r \sin\delta}\left(-\int_0^{\varphi_1} l_{xl}' \, X' d\varphi + \int_{\varphi_1}^{\pi} l_{xl} X d\varphi\right) \tag{A37}$$

The drag coefficient for specular reflection is expressed as

$$C_{D_S} = \frac{2}{\pi^{3/2} s^2 \sin\delta}\left[\int_0^{\varphi_1} l_{xd}' \left\{\beta U_x' \exp(-\beta^2 U_x'^2) - \sqrt{\pi}\,[1 - \operatorname{erf}(\beta U_x')]\left(\beta^2 U_x'^2 + \frac{1}{2}\right)\right\} d\varphi + \int_{\varphi_1}^{\pi} l_{xd}\left\{\beta U_x \exp(-\beta^2 U_x^2) + \sqrt{\pi}\,[1 + \operatorname{erf}(\beta U_x)]\left(\beta^2 U_x^2 + \frac{1}{2}\right)\right\} d\varphi\right] \tag{A38}$$

The total lift coefficient, C_{L_S}, is found by substitution of l_{xl} for l_{xd}. The values of the above integrals were found by means of numerical methods.

REFERENCES

1. Stalder, Jackson R., and Jukoff, David: Heat Transfer to Bodies Traveling at High Speed in the Upper Atmosphere. NACA Rep. 944, 1949. (Formerly NACA TN 1682)

2. Heineman, M.: Theory of Drag in Highly Rarefied Gases. Communications on Pure and Applied Mathematics, vol. 1, no. 3, Sept. 1948, pp. 259–273.

3. Ashley, Holt: Applications of the Theory of Free Molecule Flow to Aeronautics, Jour. Aero. Sci., vol. 16, no. 2, Feb. 1949, pp. 95–104.

4. Stalder, Jackson R., Goodwin, Glen, and Creager, Marcus O.: A Comparison of Theory and Experiment for High-Speed Free-Molecule Flow. NACA TN 2244, 1950.

5. Kane, E. D.: Drag Forces on Spheres in Low Density Supersonic Gas Flow. Univ. of Calif. Rep. No. HE-150-65, Feb. 15, 1950.

6. Zahm, A. F.: Superaerodynamics. Journal of the Franklin Institute, vol. 217, 1934, pp. 153–166.

7. Grimminger, G., Williams, E. P., and Young, G. B. W.: Lift on Inclined Bodies of Revolution in Hypersonic Flow, Jour. Aero. Sci., vol. 17, no. 11, Nov. 1950, pp. 675–690.

8. Mass. Inst. of Tech., Dept. of Electrical Engineering Center of Analysis. Tables of Supersonic Flow Around Cone, by the Staff of the Computing Section, Center of Analysis, under direction of Zdenek Kopal, Cambridge, 1947.

9. Loeb, Leonard B.: The Kinetic Theory of Gases. McGraw-Hill Book Co., Inc., N. Y., 2d ed., 1934.

10. Stevens, Victor I.: Hypersonic Research Facilities at the Ames Aeronautical Laboratory. Jour. of App. Physics, vol. 21, no. 11, Nov. 1950.

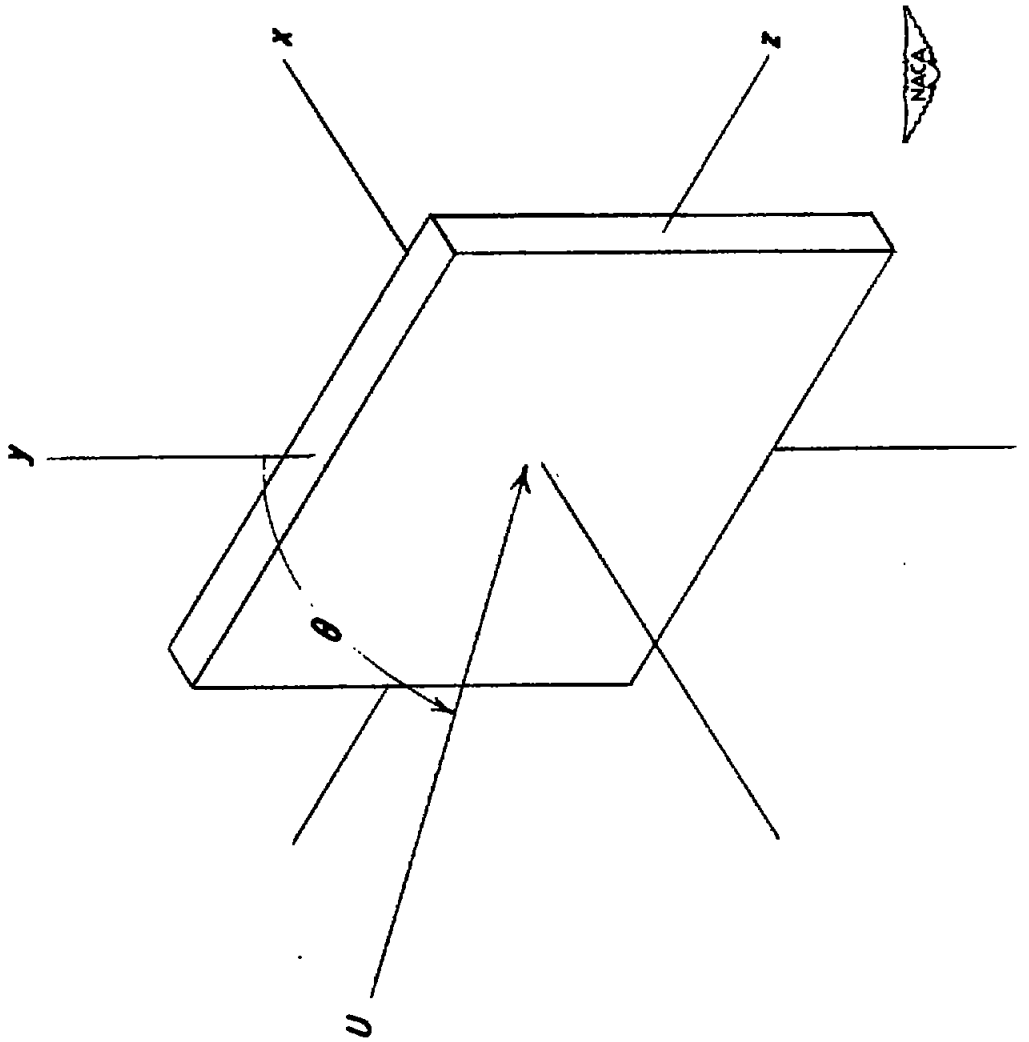

Figure 1.- Coordinate system used in analysis.

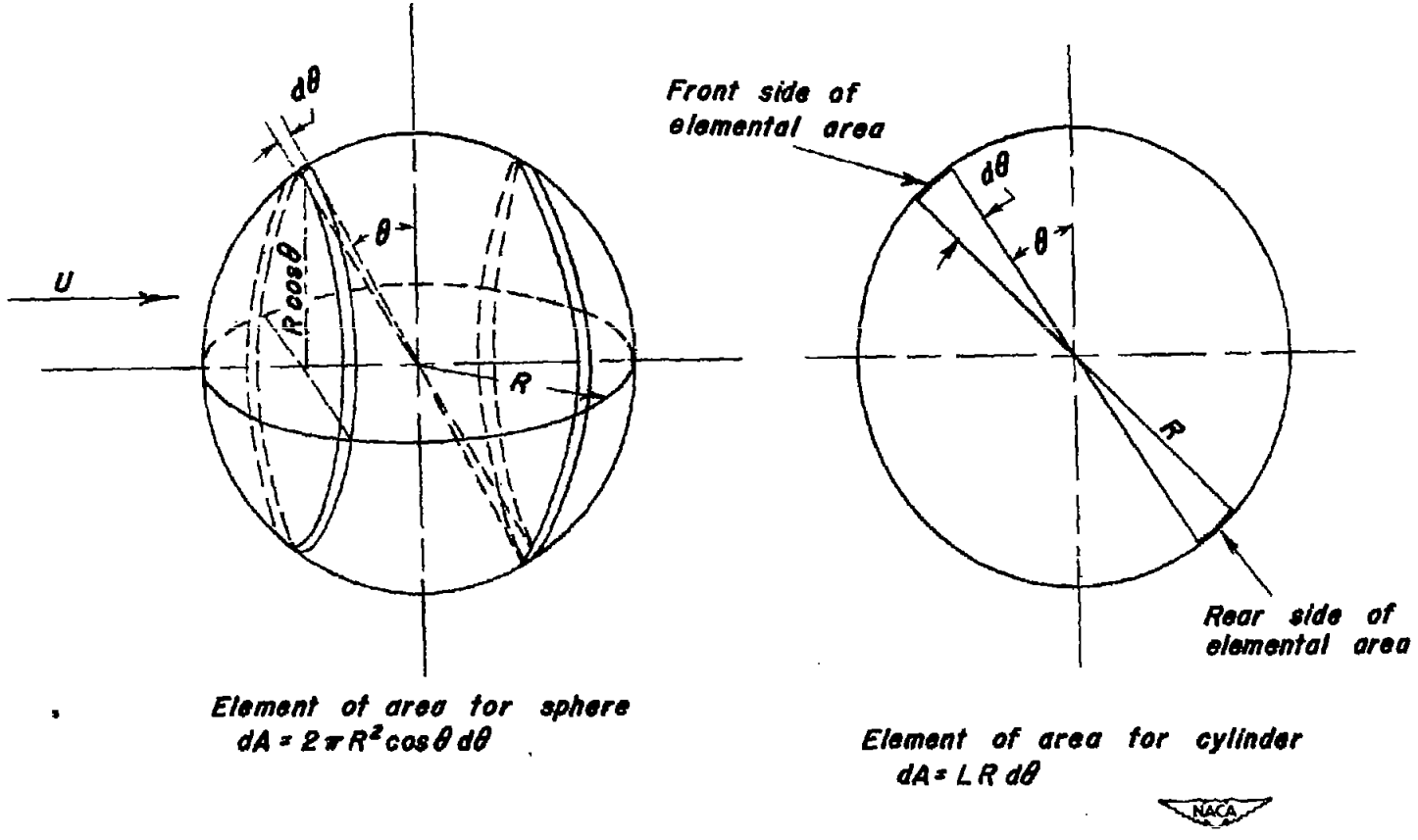

Figure 2.- Elemental areas for sphere and cylinder.

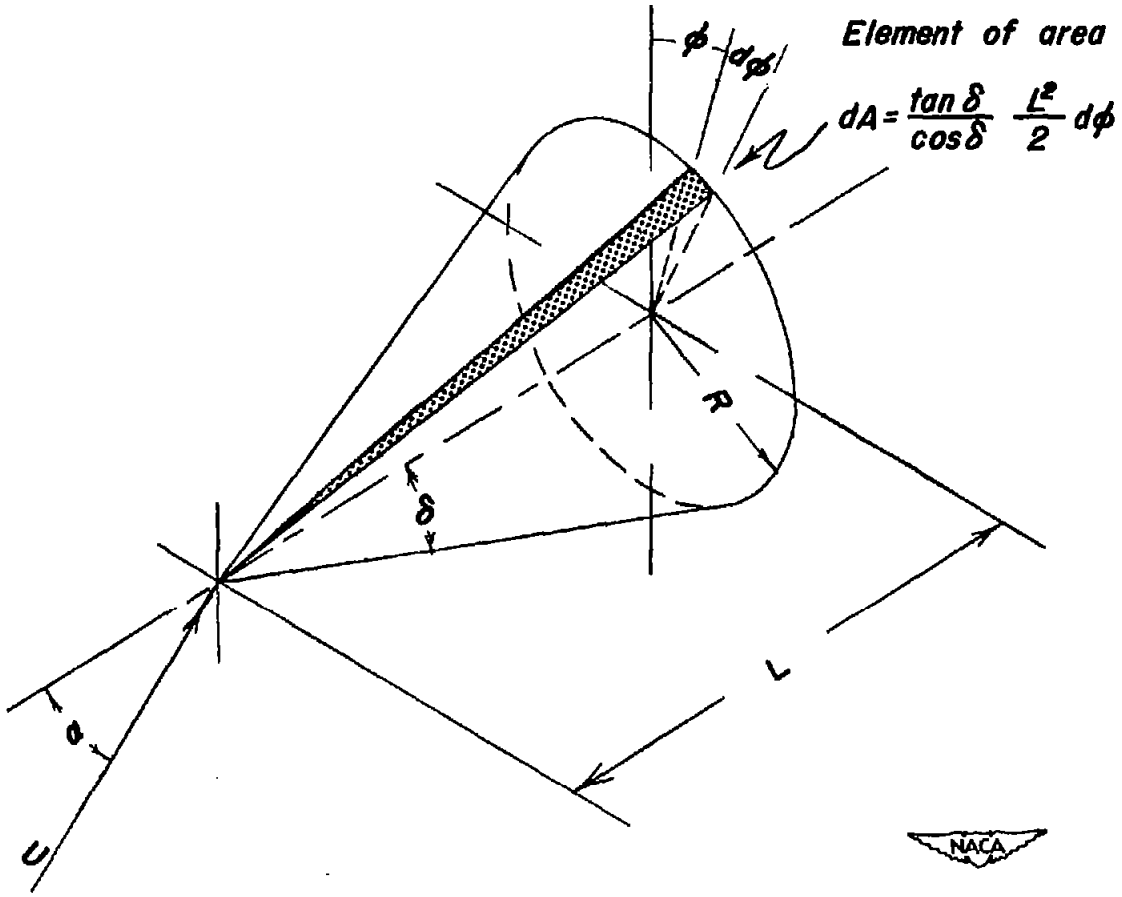

Figure 3.- Element of surface area for cone.

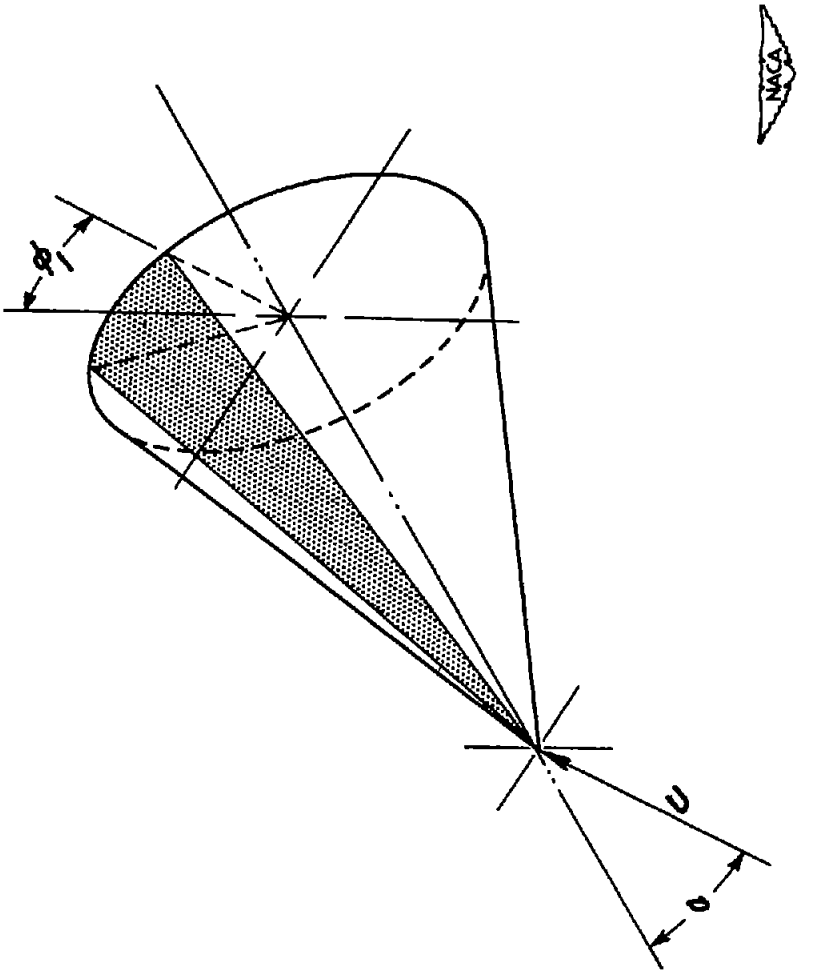

Figure 4.- Surface area shielded from mass flow.

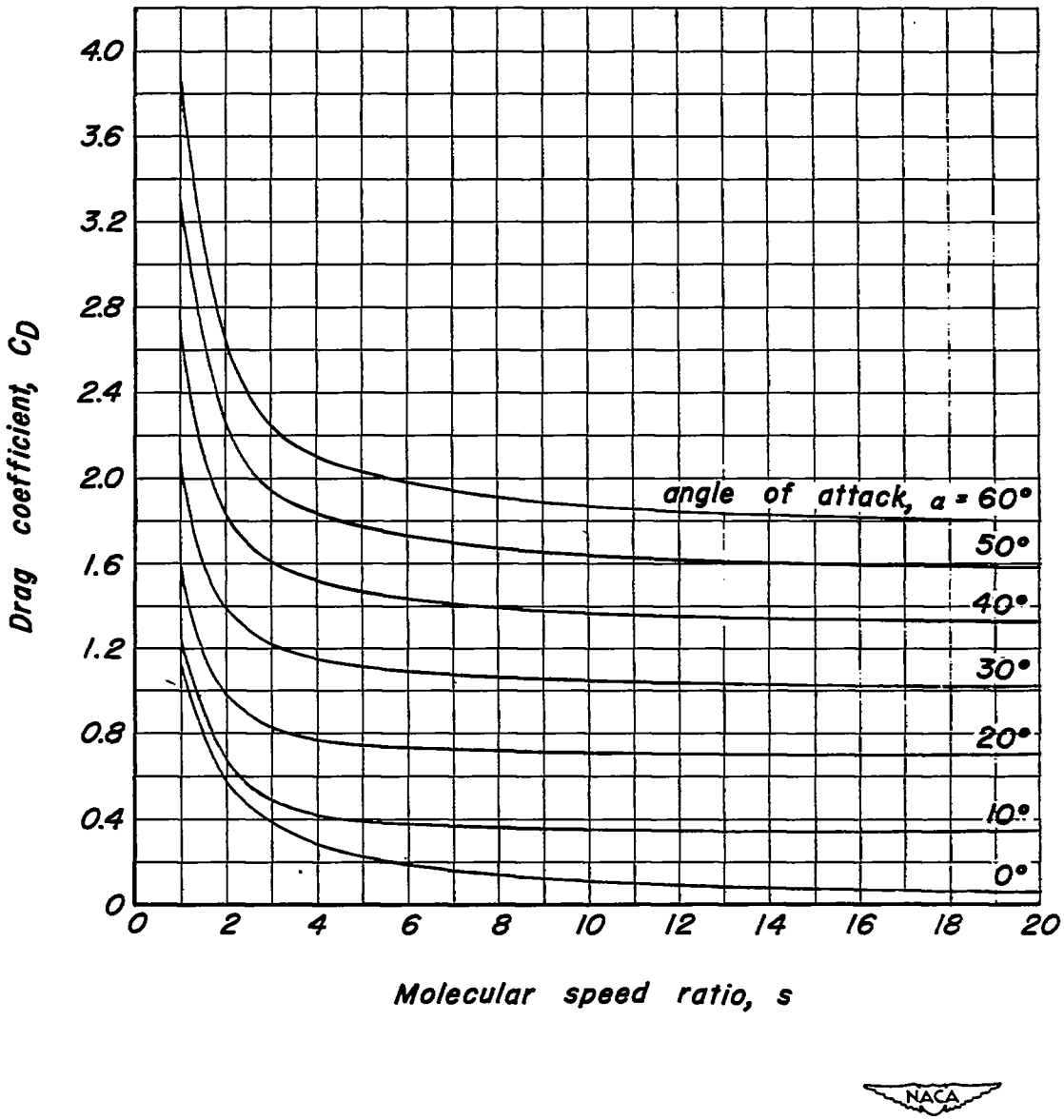

Figure 5.- Flat-plate drag coefficient, diffuse reflection.

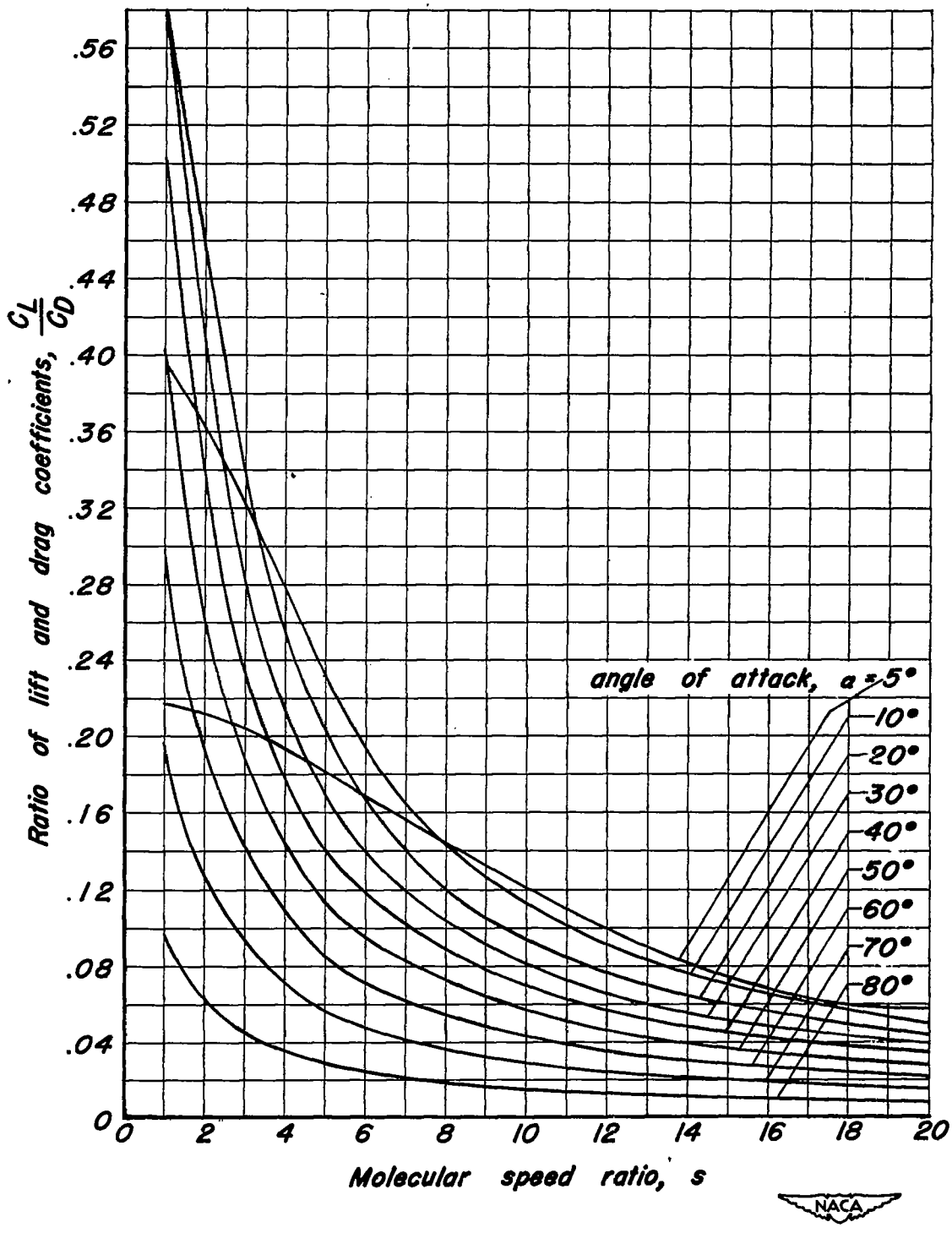

Figure 6.- Flat-plate lift-drag ratio, diffuse reflection.

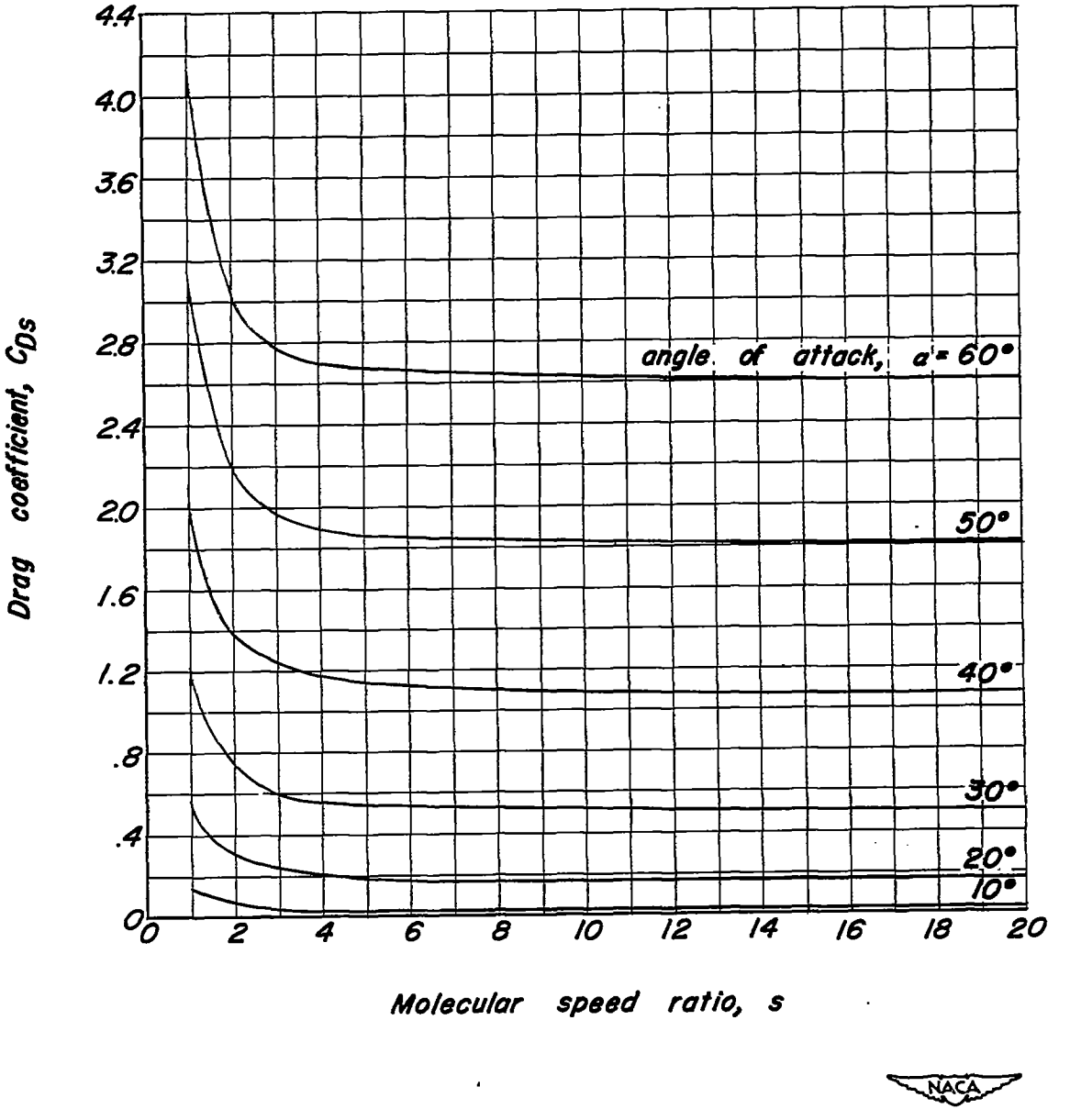

Figure 7.- Flat-plate drag coefficient, specular reflection.

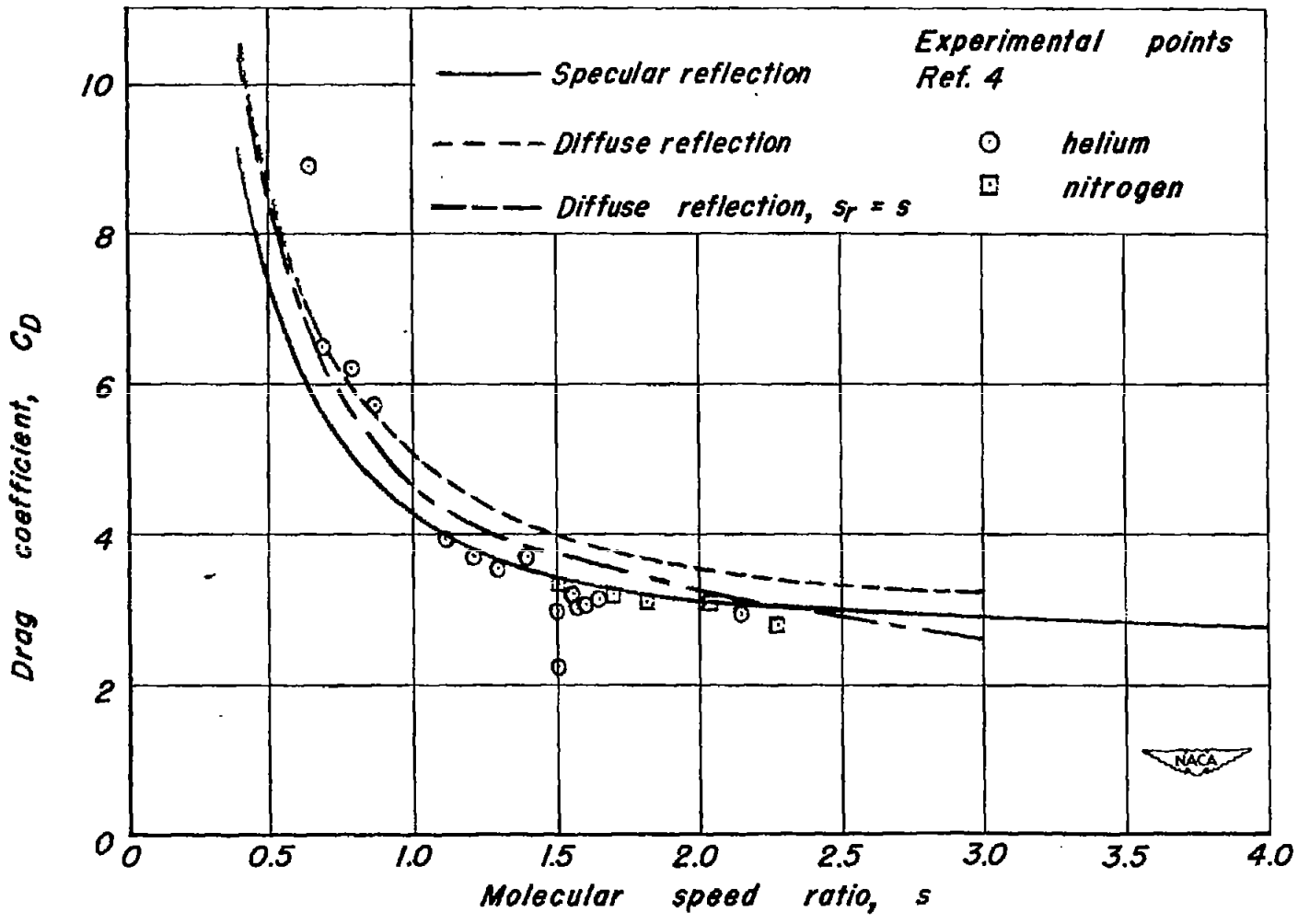

Figure 8.– Comparison of drag coefficient of cylinder for specular and diffuse reflection.

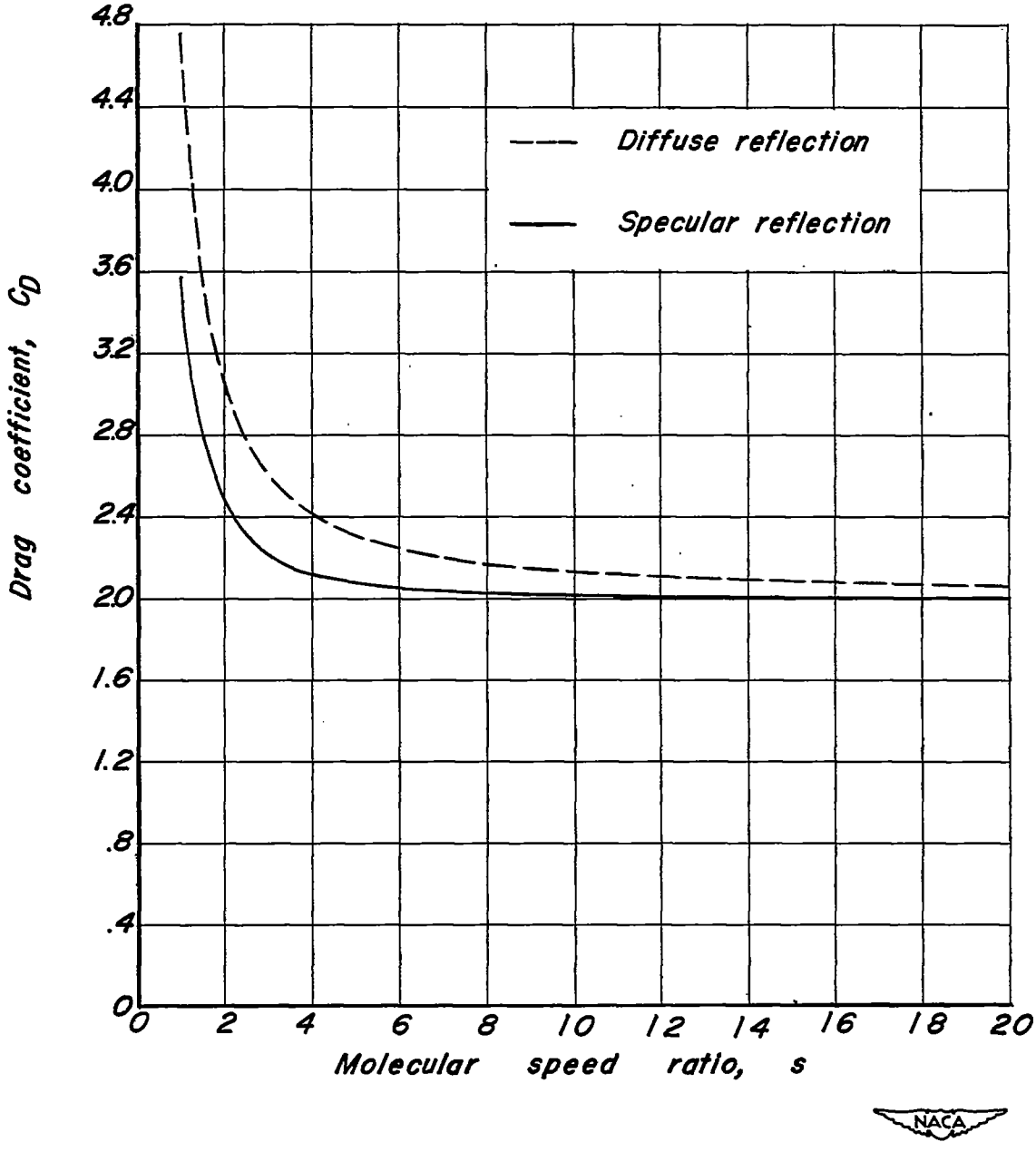

Figure 9.- Sphere drag coefficient, diffuse and specular reflection.

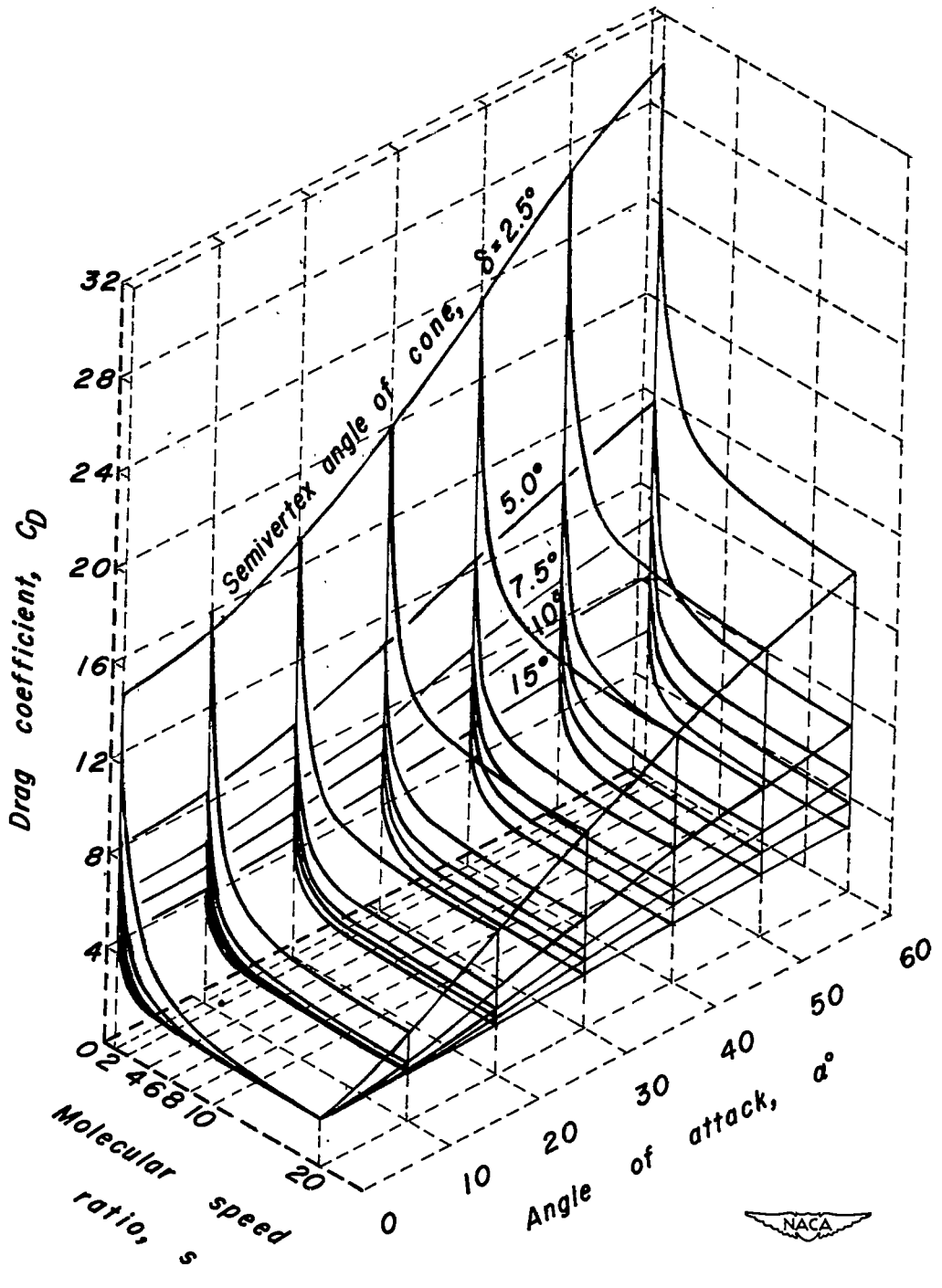

Figure 10.— Cone drag coefficient, diffuse reflection.

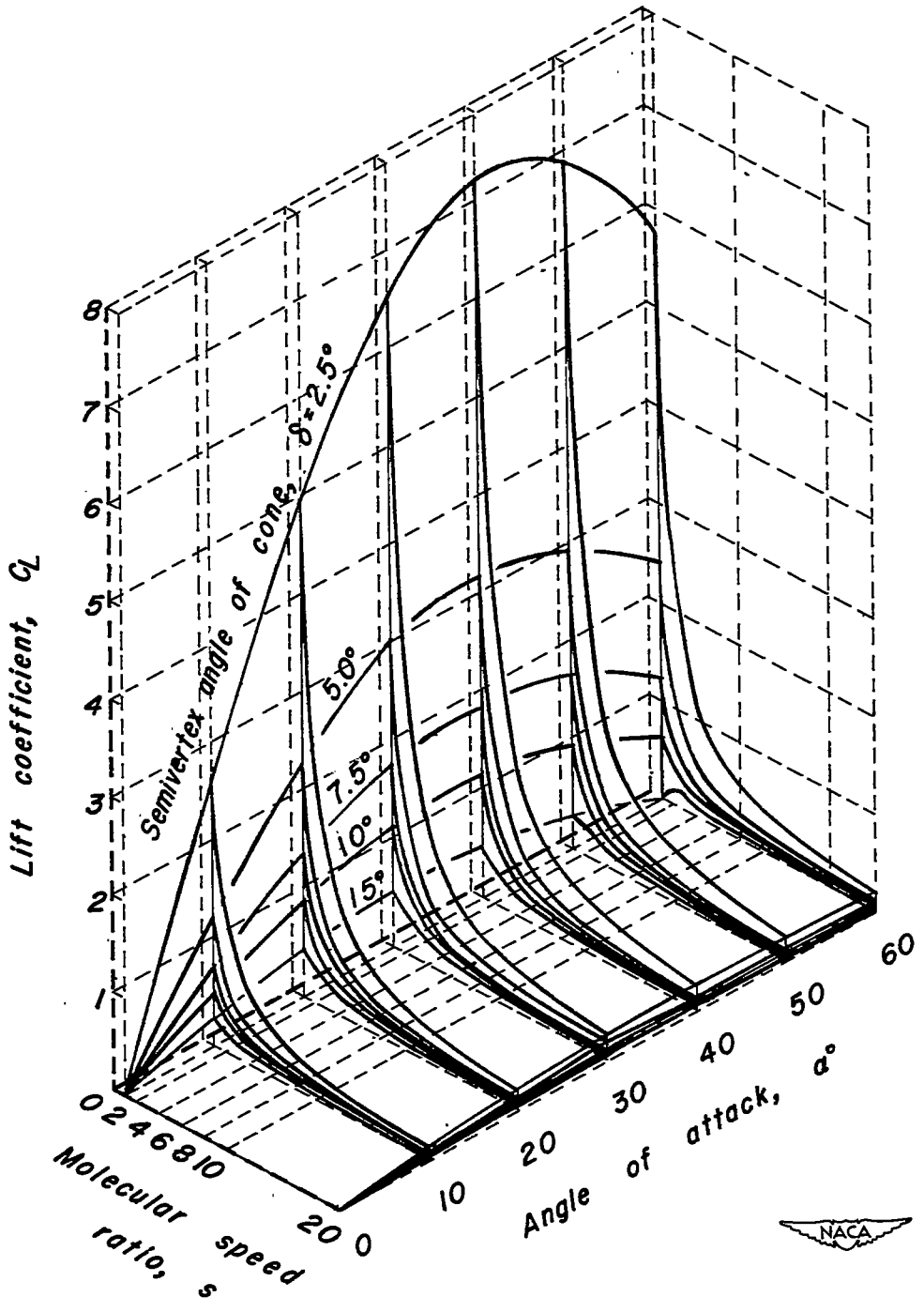

Figure 11.— Cone lift coefficient, diffuse reflection.

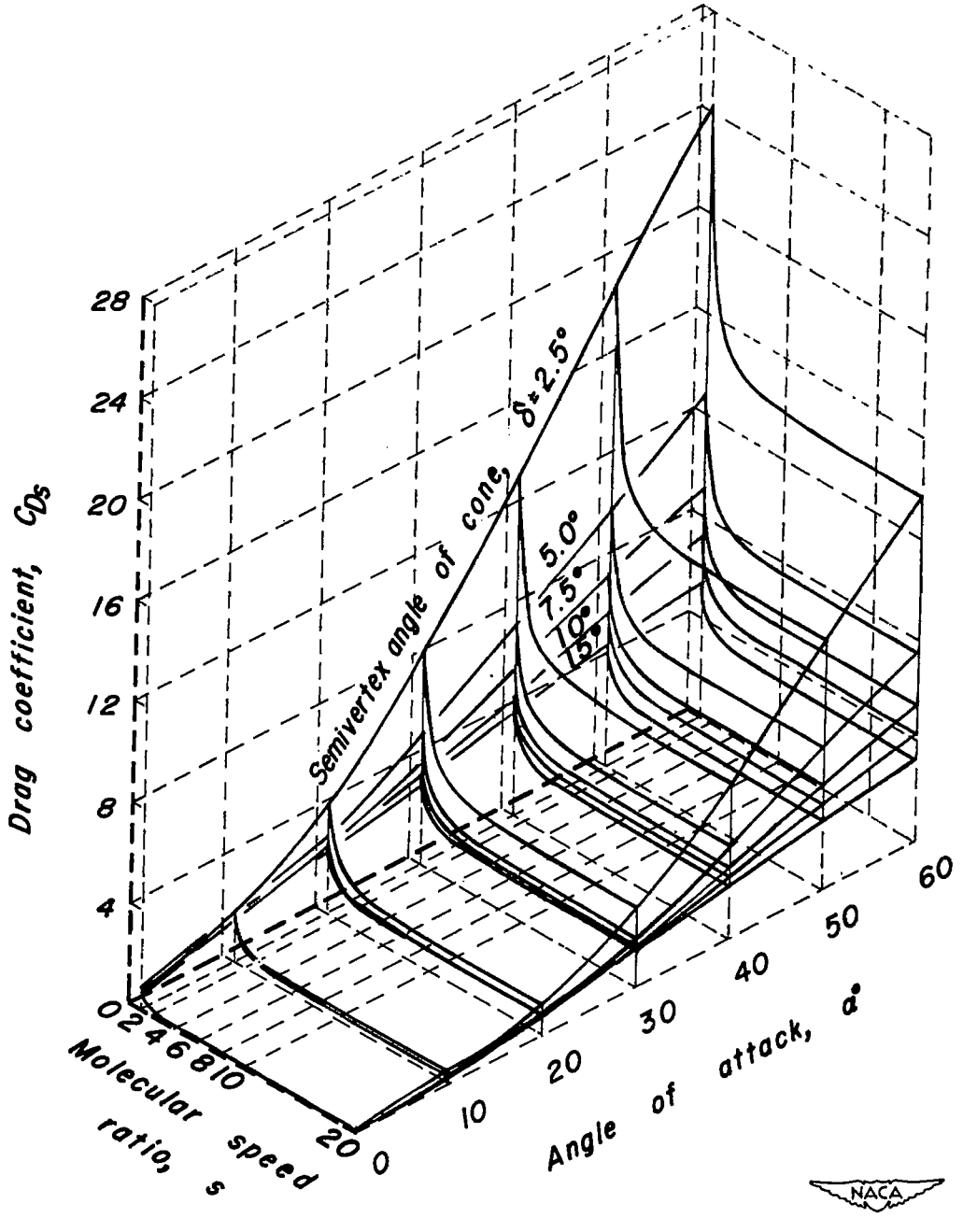

Figure 12.– Cone drag coefficient, specular reflection.

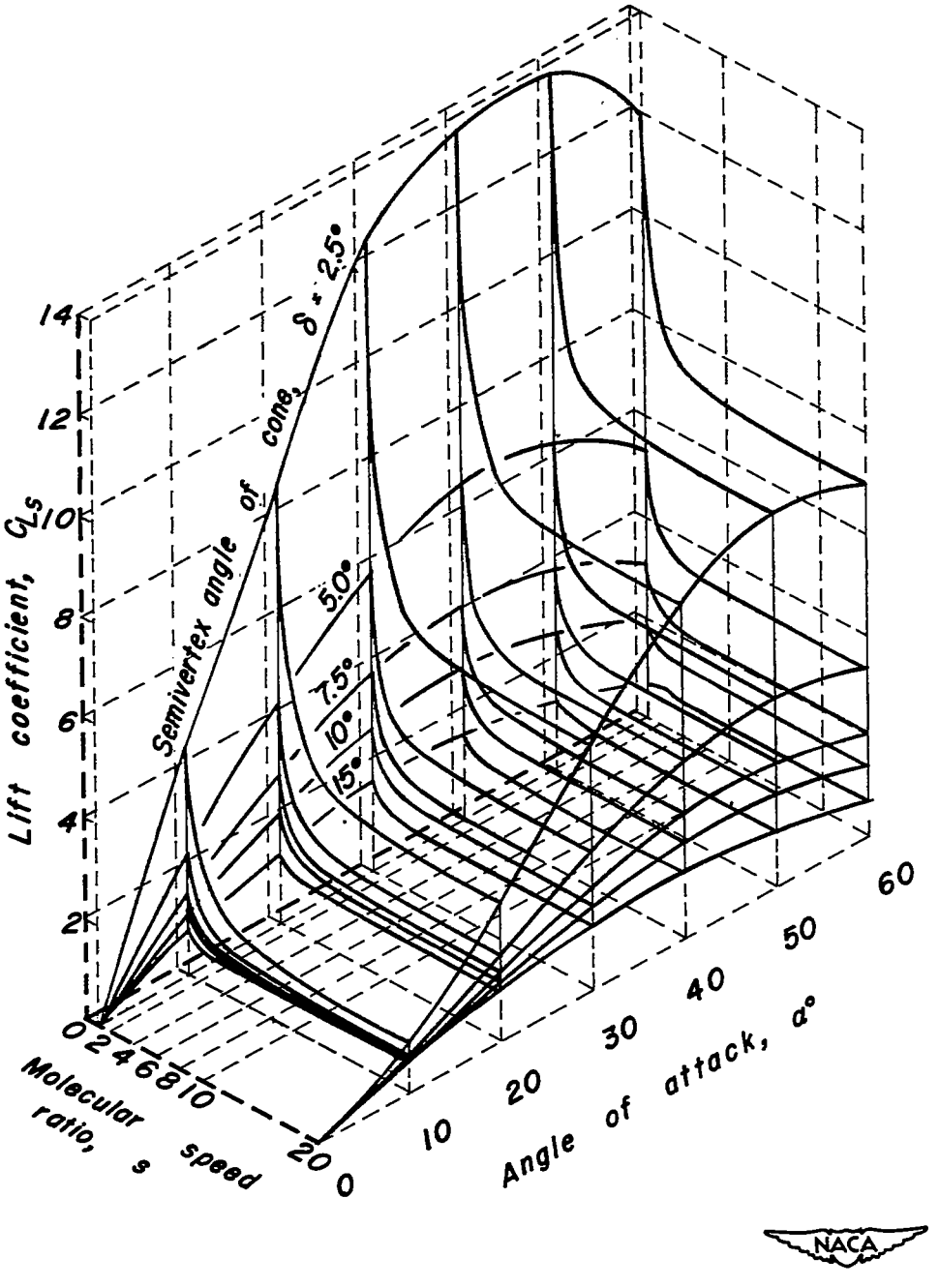

Figure 13.– Cone lift coefficient, specular reflection.

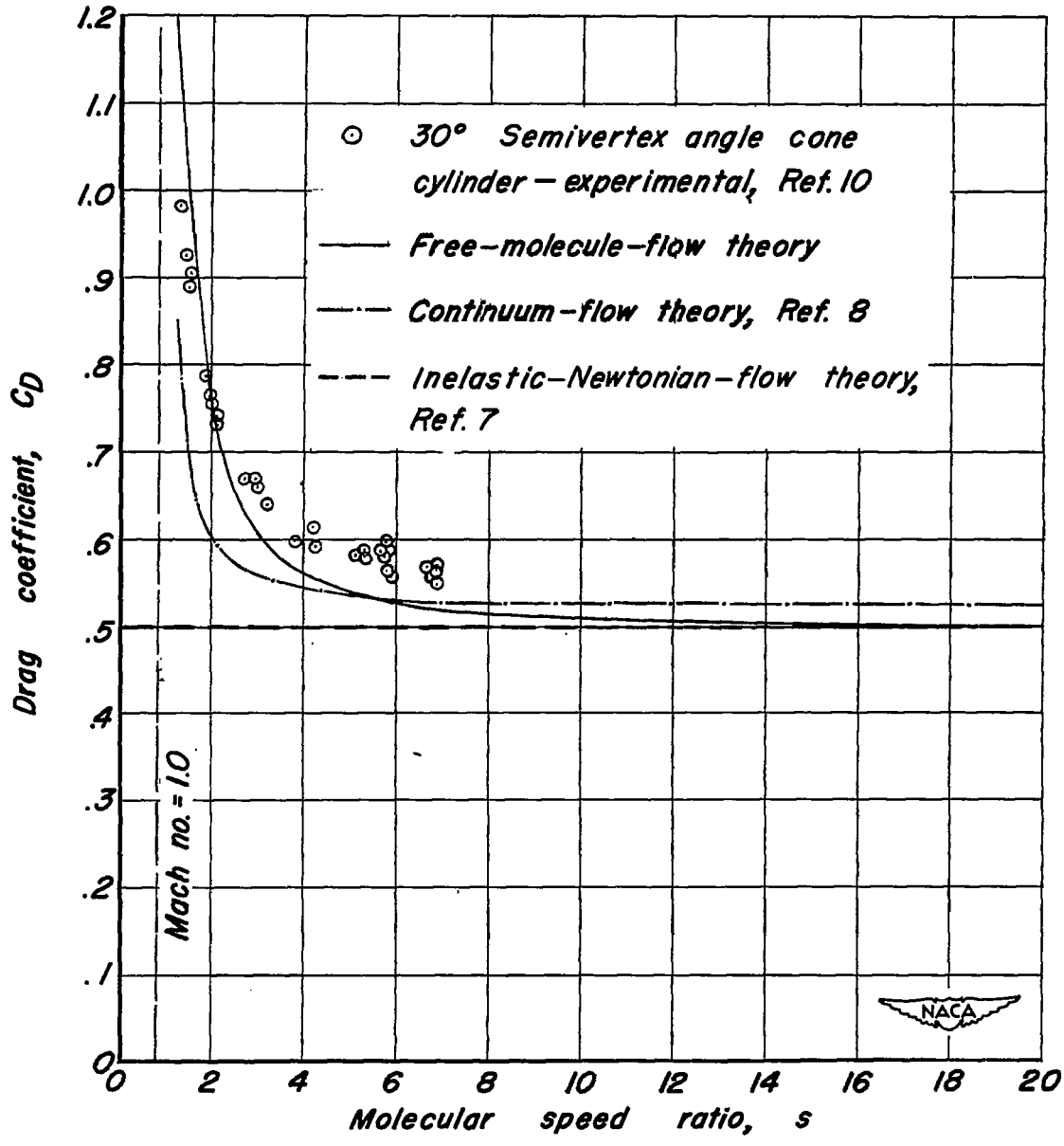

Figure 14.– Cone drag coefficient, comparison of free molecule and continuum-flow theory; $\alpha = 0°$

NACA-Langley - 7-25-51 · 1000